

Numerical Simulation of non-Newtonian Fluid Flows through Fracture Network

I A Dharmawan¹, R Z Ulhag¹, C Endyana² and M Aufaristama^{1,3}

¹ Department of Geophysics, Universitas Padjadjaran, Indonesia

² Faculty of Geology, Universitas Padjadjaran, Indonesia

³ Institute of Earth Sciences, University of Iceland, Sturlugata 7, Reykjavik 101, Iceland

E-mail: iad@geophys.unpad.ac.id

Abstract. We present a numerical simulation of non-Newtonian fluid flow in a two-dimensional fracture network. The fracture is having constant mean aperture and bounded with Hurst exponent surfaces. The non-Newtonian rheology behaviour of the fluid is described using the Power-Law model. The lattice Boltzmann method is employed to calculate the solutions for non-Newtonian flow in finite Reynolds number. We use a constant force to drive the fluid within the fracture, while the bounceback rules and periodic boundary conditions are applied for the fluid-solid interaction and inflow outflow boundary conditions, respectively. The validation study of the simulation is done via parallel plate flow simulation and the results demonstrated good agreement with the analytical solution. In addition, the fluid flow properties within the fracture network follow the relationships of power law fluid while the errors are becoming larger if the fluid more shear thinning.

1. Introduction

The study of fluid flow through fracture system is encountered in many industrial problems, such as solute transport problem [1, 2], enhanced oil recovery (EOR) [3] and many more. Solute transport in rock fractures are great attention for environmental problems, for instance remediation of contaminated of groundwater flow. In EOR processes, the non-Newtonian fluids like polymer and surfactant are play important roles to enhance the oil productivity. In those cases, the analytical solutions do not exist due to the complexity of the flow, hence the numerical simulation is promising tool to estimate the physical behavior of the system.

We employed a lattice Boltzmann method (LBM) for the simulation of non-Newtonian fluids. Recently, LBM has long standing good achievements for solving Navier-Stokes equations including heat transfer problems [4]. Compared with other traditional method like finite difference and finite element method, LBM is based on kinetic theory approach, hence it has some advantages especially when we deal with some complicated transport system in complex geometries [5]. On the other hand, LBM algorithm is also easy for parallel computation [6].

In this paper, a non-Newtonian fluid based on LBM model will be implemented in a fracture network. The power law rheology model is used to describe the non-Newtonian properties of the fluid [8, 9]. The self-affine fracture network was generated by performing fractional Brownian Motion (fBM) method which proposed by Madadi et al [7]. Hence, it can capture the surface roughness of the natural fracture by including the fractal dimension. While, the LBM simulations of Newtonian flow for this system has been clearly discussed in [10, 11, 12]. The objective of



the present work is to analyse numerically of the flow velocity, shear stress and viscosity and its dependence on the fluid rheology and the fracture geometry effect.

2. The lattice Boltzmann method

The LBM method was developed as an alternative tool for Computational Fluid Dynamics. LBM consists of discrete particles with particular velocities. The particle distribution functions is defined as $f_i(\vec{x}, t)$, where \vec{x} and t is position vector and time, respectively. The subscript i is the lattice link of the distribution function. During simulation, the particles will propagate and collide in a regular lattice. The distribution functions will evolve and interact in such way that that mass, momentum and energy are conserved.

The evolution equation of the LBM is defined as [13]

$$f_i(\vec{x} + \vec{c}_i \Delta x, t + \Delta t) = f_i(\vec{x}, t) + \Omega_i(\vec{x}, t) \quad (1)$$

Here, in this paper we consider D2Q9 lattice, where D2 indicates for two dimension and Q9 indicates for nine velocity vectors. The discrete velocities for this lattice are the following

$$\begin{aligned} \vec{c}_i &= (0, 0); \quad i = 0 \\ \vec{c}_i &= \cos\left(\frac{\pi}{2}(i-1)\right), \sin\left(\frac{\pi}{2}(i-1)\right); \quad i = 1, 2, 3, 4 \\ \vec{c}_i &= \sqrt{2} \cos\left(\frac{\pi}{2}(i-1) + \frac{\pi}{4}\right), \sin\left(\frac{\pi}{2}(i-1) + \frac{\pi}{4}\right); \quad i = 5, 6, 7, 8 \end{aligned} \quad (2)$$

The Ω_i is the collision operator. For this simulation, we use Bhatnagar-Gross-Krook collision operator [14]

$$\Omega_i = \frac{-1}{\tau} [f_i(\vec{x}, t) - f_i^{eq}(\vec{x}, t)] \quad (3)$$

while τ is the time of relaxation. The equilibrium distribution function f_i^{eq} is given by

$$f_i^{eq}(\vec{x}, t) = \omega_i \rho \left(1 + 3\vec{c}_i \cdot \vec{u} + \frac{9}{2} (\vec{c}_i \cdot \vec{u})^2 - \frac{3}{2} \vec{u}^2 \right) \quad (4)$$

where $\omega_0 = \frac{4}{9}$ for $i = 0$, $\omega_1 = \frac{1}{9}$, for $i = 1, 2, 3, 4$ and $\omega_i = \frac{1}{36}$ for $i = 5, 6, 7, 8$. The macroscopic fluid parameters like fluid density ρ and velocity \vec{u} can be calculated from the distribution functions at each node by

$$\rho = \sum_i f_i \quad \text{and} \quad \rho \vec{u} = \sum_i f_i \vec{c}_i \quad (5)$$

The kinematic viscosity is related with relaxation time, which defined as

$$\nu = \frac{1}{3} \left(\tau - \frac{1}{2} \right) \quad (6)$$

The relation between stress tensor $\sigma_{\alpha\beta}$ and the strain rate tensor $D_{\alpha\beta}$ for incompressible fluid is given by

$$\sigma_{\alpha\beta} = 2\mu D_{\alpha\beta} \quad (7)$$

The local viscosity μ is the a function of the invariants of the strain rate tensor. Here we use power law fluids, the viscosity is defined as

$$\mu = m \dot{\gamma}^{n-1} \quad (8)$$

where m and n are some constants, when $n > 1$ the fluid is categorized as shear-thickening fluid, when $0 < n < 1$ is categorized as shear-thinning fluid and when $n = 1$ the fluid is Newtonian. The local shear rate $\dot{\gamma}$ is then defined as

$$\dot{\gamma} = 2\sqrt{D_{\alpha\beta}D_{\alpha\beta}} \quad (9)$$

in LBM the strain rate tensor is given by

$$D_{\alpha\beta} = -\frac{3}{2\rho\tau} \sum_i (f_i - f_i^{eq}) c_{i\alpha} c_{i\beta} \quad (10)$$

which is equal with equation 7.

For the validation study, we set the pressure gradient $\nabla P = G$ in the x -direction, and with power law parameters m and $n > 0$, in a channel width d , we will have the analytical solution of the velocity as

$$u_x(y) = \frac{n}{n+1} \left(\frac{G}{m}\right)^{1/n} \left(\left|\frac{d}{2}\right|^{(n+1)/n} - \left|\frac{d}{2} - y\right|^{(n+1)/n} \right) \quad (11)$$

3. Results and Discussion

3.1. Parallel plate validaton

The LBM was implemented on parallel plate for numerical validation. Simulation were run at low Reynold's number to ensure the flow is in laminar regime. The parameter n was varied to capture the shear thinning and thickening properties. We applied the bounceback rules for solid-fluid interaction, while Zou-He boundary conditions are applied for inlet and outlet flow [15]. The results displayed in Figure 1, it showed that the numerical solutions (marked) agreed very well with the analytical solutions (solid lines) Equation 11 for different n . We set $G = 1.0 \times 10^{-6}$ and $m = 0.02$ for validation study.

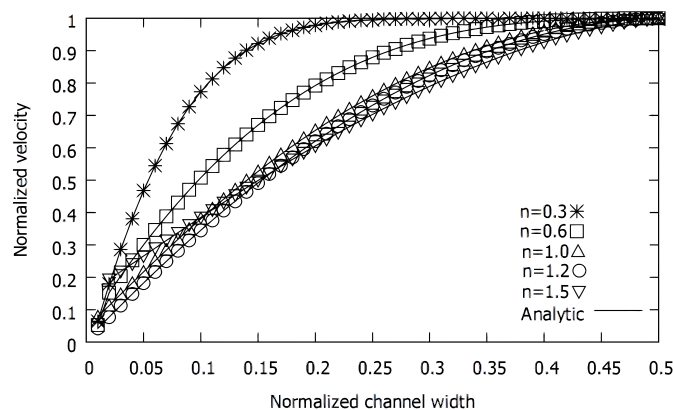


Figure 1. Velocity profile for flow in parallel plate for different n

3.2. Flow in fracture network

Our simulation are performed on the two-dimensional fracture network having size 342×680 in lattice unit. The fracture network geometry is developed using fBM method [7]. In this study we set the surface roughness $H = 0.8$ which is illustrated in Figure 2 and Figure 3. The fracture network was developed in such a way that they have same mean apertures for each branches. The power law fluid parameters are set with three different n (0.6; 1.0 1.5). Additional layer

was added in inlet and outlet in order to perform periodical boundary conditions. The steady state conditions are reached after 50 000 iterations.



Figure 2. Velocity field (a) and viscosity profile (b) for fluids flowing through the fracture network with $n = 0.6$



Figure 3. Velocity field (a) and viscosity profile (b) for fluids flowing through the fracture network with $n = 1.5$

Figure 2 presents velocity and viscosity distribution for shear thinning ($n = 0.6$) fluid. The velocity profile has power-law fluid with viscosity, i.e. the higher shear rate, the lower viscosity. The red colour indicates the higher value while the blue is lower, this means the fluid will preferably flow in non-blue regions. In shear thickening fluid, the relationship between the velocity and viscosity is vice versa with the previous case as shown in Figure 3. This corresponds very well with the relationships of power law fluid. We then calculate the fluid flux for different constant pressure gradient. The slopes are tabulated in Table 1 and the plot is shown in Figure 4.

Table 1. Slopes from plots of $\log[u]$ vs. $\log[G]$

n	$1/n$	slope	% Error
0.6	1.6667	1.35576	0.18
1	1.0000	1.0000	0.00
1.5	0.6667	0.6667	0.00

Figure 4 shows the plot of $\log[u]$ versus $\log[G]$ for this simulation with different n . The error for Newtonian and shear thickening flow is less than 1%. Error increases with decreasing n or

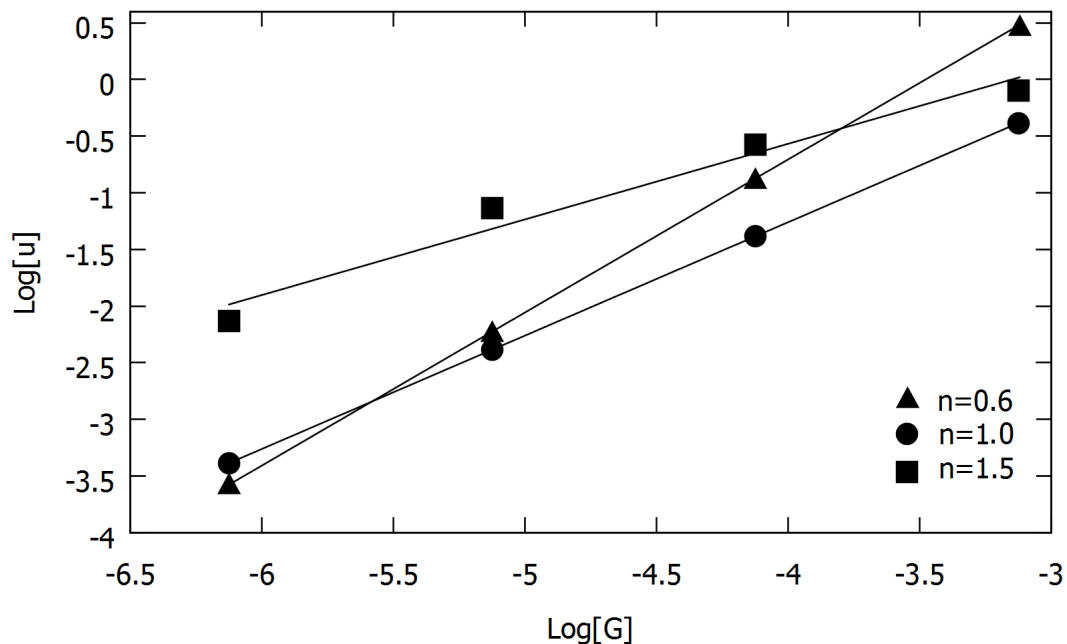


Figure 4. Logarithmic plot for the flow rate ($\log[u]$) versus pressure difference ($\log[G]$) for non-Newtonian flow with different n

fluid become more shear thinning. In power-law fluid model the problem may arise if the local strain-rate produces very small number or even zero, this only happen when $n < 1$ because the local viscosity will grows up into very huge number and then we get inaccuracy results. On the other hand, the strain rate in shear thickening fluid is more distributed within the fracture and the local viscosity produces moderate values.

4. Conclusion

The power law non-Newtonian fluid flow in fracture network was studied numerically using lattice Boltzmann method. The flow rate through the fracture network is linear proportional to the logarithmic applied pressure difference. The Newtonian and shear thickening flow produced consistent results with theory, while for shear thinning flow the low shear rates contribute to the inaccuracy results.

Acknowledgment

The calculations were performed at the Guriang Computer Cluster <http://guriang.unpad.ac.id>. This work was financed by Directorate Degree for Higher Education (DIKTI) contract no 393/UN6.R/PL/2015.

References

- [1] Yeo I W 2001. *Geosciences Journal* **5** 2.
- [2] Dou Z and Zhou Z F 2014. *Water Science and Engineering* **7** 3.
- [3] Hatiboglu C U and Tayfun 2007. *Phys. Rev. E* **76** 6.
- [4] Shiyi C and Doolen G D 1998. *Annu. Rev. Fluid.* **30** 1.
- [5] Succi S, Foti E and Higuera F 1989. *Europhys. Lett.* **10** 5.
- [6] Mazzeo M D and Coveney P V 2008. *Comp. Phys. Comm.* **178** 12.
- [7] Madadi M, VanSiclen V D and Sahimi M 2003. *Journal of Geophysical Research* **108** 2396.
- [8] Aharonov E and Rothman D H 1993. *Geophys. Res. Lett* **20** 679.

- [9] Boyd J, Buick J and Green S 2006. *J. Phys. A: Math. Gen.* **39** pp 14241-7.
- [10] Drazer G and Koplik J 2000. *Phys. Rev. E.* **62** 6.
- [11] Madadi M and Sahimi M 2003. *Phys. Rev. E* **67** 026309.
- [12] Eker E and Akin S 2006. *Transport in Porous Media* **65**: pp 363-84.
- [13] Chen S and Doolen G D 1988. *Ann. Rev. of Fluid Mechanics* **30** pp. 329-64.
- [14] Bhatnagar P L, Gross E P and Krook M 1954. *Phys. Rev.* **511**.
- [15] Zou Q and He X 1997. *Phys. Fluids* **9** 1591.